*Journal of Sound and Vibration, 2004*

# Time Reversal Active Sensing for Health Monitoring of a Composite Plate

Hyun Woo Park[1], Hoon Sohn[2)*], Kincho H. Law[1], and Charles R. Farrar[2]

[1] Department of Civil and Environmental Engineering

Stanford University, California 94305, USA

[2] Engineering Sciences and Applications Division, M/S T006

Los Alamos National Laboratory, New Mexico 87545, USA

**ABSTRACT**

This study investigates the applicability of time reversal concept in modern acoustics to structural health monitoring. A time reversal method has been adapted to guided-wave propagation to improve the detectability of local defects in composite plate structures. Specifically, wavelet-based signal processing techniques have been developed to enhance the time reversibility of Lamb wave in thin composite plates. The validity of the proposed method is demonstrated through experimental studies in which input signals exerted at piezoelectric (PZT) patches on a quasi-isotropic composite plate are successfully reconstructed using the time reversal method. The development presented here will allow some progress in in-service monitoring of aerospace, automotive, civil, and mechanical systems.

## 1. INTRODUCTION

There has been a significant increase in using solid composites in load-carrying structural components, particularly in aircraft and automobile industries. With the advances in sensor and hardware technologies that can generate and detect Lamb waves, many studies have been proposed to use Lamb waves for detecting defects in composite structures [1,2,3,4]. In particular,

---

* Auhtor to whom correspondence should be addressed. E-mail: sohn@lanl.gov.

many researchers have recognized the potential use of PZT actuators/sensors for Lamb wave based structural health monitoring. [2,4,5].

Lamb waves are mechanical waves whose wavelength is in the same order of magnitude as the thickness of the plate. The analysis and interpretation of Lamb waves can be complicated due to their dispersive and multimodal natures. The various frequency components of Lamb waves travel at different speeds and the shapes of wave packets change as they propagate through a solid medium. Multiple symmetric and anti-symmetric wave modes are generated as the driving frequency for wave generation increases.

Recently, attention has been paid to the time reversal method developed in modern acoustics to compensate the dispersion of Lamb waves and to improve the signal-to-noise ratio of propagating waves [6,7,8,9]. Though the experimental results showed the spatial focusing and time compression properties of time reversal Lamb waves, the results were not directly usable for damage detection of plates [8]. Instead, a pulse-echo time reversal method, that is, the time reversal method working in pulse echo mode has been employed to identify the location and size of defects in a plate [7,8,9]. In the pulse-echo time-reversal method, Lamb waves are generated by a tuneburst input and the associated responses are recorded by an array of sensors, called *a time reversal mirror,* surrounding the plate boundary. If there is any defect along the wave propagation paths, echoes are produced by the defect and recorded by the time reversal mirror. The recorded echoes are then reversed in a time domain and reemitted by the same time reversal mirror, which acts as an actuator array this time. As the reemitted signals converge on the defect location, amplified echo signals will be produced by the defect. By iterating this pulse-echo time-reversal process, the identification of the defect can be improved. However, if there exist multiple defects in a plate, this iterative pulse-echo process tends to detect only the most distinct defect, requiring more sophisticated techniques to detect multiple defects. Furthermore, the pulse-echo process seems impractical for structural health monitoring applications, because a dense array of sensors is required to cover the entire boundary of the plate being investigated.

In this study, an enhanced time reversal method is proposed to utilize time reversal Lamb waves directly for damage detection of plates. In the enhanced time reversal method, an input signal can be reconstructed at an excitation point (point A) if an output signal recorded at another point (point B) is reemitted to the original source point (point A) after being reversed in a time domain as shown in Figure 1. This time reversibility of waves is based on the spatial reciprocity and time-reversal invariance of linear wave equations [10,11]. The uniqueness of the enhanced time reversal method lies in the development of signal-processing techniques that extend the conventional time reversal acoustics, which is applicable only to body waves, to Lamb waves. In particular, a specific input waveform and a wavelet-based signal filtering technique are employed to enhance the time reversibility of Lamb waves. When it comes to damage detection, damage causes wave distortions due to wave scattering and it breaks down the linear reciprocity of the wave propagation. Simultaneous actuation and sensing needed for the enhanced time reversal method can be readily implemented in the current active PZT sensing system in which multiple defects in a plate can be detected. The validity of the proposed method is demonstrated through the experimental studies of a quasi-isotropic composite plate, in which input signals exerted at PZT patches are successfully reconstructed during the time reversal process.

This paper is organized as follows: First, an analysis of Lamb waves using the Mindlin plate theory is described in Section 2. In Section 3, the time reversibility of Lamb waves is investigated by introducing a time reversal operator in a frequency domain. The wavelet-based signal processing techniques to enhance the time reversibility of Lamb waves are discussed in

Section 4. A numerical example and experimental investigations are presented in Section 5 to demonstrate the validity of the enhanced time reversal method. Finally, this paper is concluded in Section 6 with a brief summary and discussions.

## 2. LAMB WAVES IN A COMPOSITE PLATE

Lamb waves usually occur on the waveguides such as bars, plates and shells. Unlike body waves, the propagation of Lamb waves is complicated due to two unique features: dispersion and multimode [12]. Theoretically, these two features can be investigated by solving Rayleigh-Lamb equations defined for the symmetrical and anti-symmetrical modes on an infinite plate with a thickness $h$.

$$(k^2 + s^2)\cosh(qh)\sinh(sh) - 4k^2 qs\sinh(qh)\cosh(sh) = 0 \tag{1a}$$

$$(k^2 + s^2)\sinh(qh)\cosh(sh) - 4k^2 qs\cosh(qh)\sinh(sh) = 0 \tag{1b}$$

where $q^2 = k^2 - k_l^2$ and $s^2 = k^2 - k_t^2$. Furthermore, $k$ denotes a wave number, and $k_l$ and $k_t$ are the wave numbers for the longitudinal and shear modes, respectively. It should be noted that there exist multiple wave modes that satisfy Equation (1a). The dispersion curve can be expressed in terms of the product of the excitation frequency and the plate thickness versus the group velocity $C_g$, which is defined as:

$$C_g = \frac{d\omega}{dk} \tag{2}$$

where ω denotes an angular frequency. For a uniform plate with constant thickness, the dispersion curve can be represented as a function of the frequency as shown in Figure 2.

As shown in Figure 2, multiple Lamb wave modes are created as the excitation frequency increases. The dispersive nature of waves causes the different frequency components of Lamb waves to travel at different speeds and the shape of the wave packet to change as it propagates through a solid medium. Due to the dispersive and multimodal characteristics of Lamb waves, it is difficult to analyze the wave signals and to identify existence of damage. Therefore, two fundamental modes, namely the first symmetrical $S_0$ mode and anti-symmetrical $A_0$ mode are often selected and generated for damage detection applications because these modes are less sensitive to dispersion than other higher modes. For the layout of the PZT actuators and sensors as discussed in Section 5, the magnitude of $S_0$ mode is rather small and negligible compared to that of $A_0$ mode [2]. The discussion below focuses only on the $A_0$ mode.

The exact solution of the Lamb-Rayleigh equations (1a) can be quite complicated. Here, approximate wave equations based on the Mindlin plate theory are employed to predict the wave propagation of the $A_0$ mode and to validate the experimental results [5]. In the Mindlin plate theory, the Navier-Cauchy equations of three-dimensional elasticity for a plate is idealized and simplified in terms of a deflection and two rotations along the neutral plane of the plate. Particularly, the Mindlin plate theory can be used for predicting the $A_0$ mode propagating on a quasi-isotropic composite plate if the effective transverse-shear modulus is determined appropriately [13].

When an arbitrary PZT patch A is used as an actuator and another distinct PZT patch B is used as a sensor as shown in Figure 3, the response voltage at the sensing PZT patch B can be represented as follows:

$$\hat{V}_B(r,\omega) = K_s(\omega)\hat{\mathrm{E}}_B(r,\omega) \tag{3}$$

where, $r$, $\hat{V}_B$, $K_s$, and $\hat{\mathrm{E}}_B$ are a wave propagation distance from the center of the actuating PZT patch to the sensing PZT patch, a response voltage at the sensing patch B, a mechanical-electro efficiency constant, and surface strain at the center of the patch B with respect to the angular frequency $\omega$, respectively.

The surface strain at the patch B can be rewritten as follows.

$$\hat{\mathrm{E}}_B(r,\omega) = \hat{I}_A(\omega)K_a(\omega)G(r,\omega) \tag{4}$$

where, $\hat{I}_A$, $K_a$ and $G$ are an input voltage at the patch B, a counterpart of mechanical-electro efficiency $K_s$ in Eq (3), and an impulse response function of the patch B as a result of the input at the patch A, respectively. Specifically, the impulse response function $G$ is obtained by applying Hankel and inverse Hankel transform in the spatial domain and Fourier transform in the time domain into the wave equations based on the Mindlin plate theory [13].

$$G(r,\omega) = -\frac{i\pi h^2}{8D}\frac{\gamma_1 k_1^3 a \mathrm{J}_1(k_1 a)\mathrm{H}_0^{(1)}(k_1 r)}{k_1^2 - k_2^2} \tag{5}$$

where $D$, $\gamma_1$, $a$, $\mathrm{J}_1(\cdot)$ and  are the flexural stiffness of the plate, the ratio of dilatational wave to vertical wave motion of the plate at the wave number $k_1$, the radius of PZT patch A, the first order Bessel function, and the zeroth order Hankel function of first kind, respectively. The wave numbers, $k_1$ and $k_2$ determined at the $A_0$ mode and the second flexural $A_1$ mode of the plate, respectively. The propagation of the $A_0$ mode can be numerically simulated using Eq.(4). Later on this numerical prediction will be compared with experimental results.

## 3. TIME REVERSAL LAMB WAVES IN A COMPOSITE PLATE

The origin of the time reversal method traces back to the time reversal acoustics [9,11]. In time reversal acoustics, an input body wave can be exactly reconstructed at the source location if a response signal measured at a distinct location is time-reversed (literally the time point at the end of the response signal becomes the starting time point) and reemitted to the original excitation location. This phenomenon is referred to as time reversibility of body waves and has found applications in lithotripsy, ultrasonic brain surgery, nondestructive evaluation, and acoustic communications [9].

While the time reversal method for non-dispersive body waves in fluids has been well-established, the study of the time reversal method for Lamb waves on plates is still relatively new. Because of the dispersion characteristic of Lamb waves, wave packets traveling at higher speeds arrive at a sensing point earlier than those traveling at lower speeds. However, during the time reverse process at the sensing location, the wave packets, which travel at slower speeds and arrive at the sensing point later, are reemitted to the original source location first. Therefore, all wave packets traveling at different speeds concurrently converge at the source point during the time reversal process, compensating the dispersion. The application of the time reversal method to Lamb wave propagation can compensate the dispersion effect, which has limited the use of Lamb waves for damage detection applications [7,8]. The effect of dispersion on the time reversal analysis of Lamb waves in a homogeneous plate was first studied by Wang et. al [5] by introducing the time reversal operator into the Lamb wave equation based on the Mindlin plate theory.

While a number of experimental evidences have shown that the dispersion of Lamb waves is well compensated through the time reversal process, the time reversibility of Lamb waves has not been fully investigated unlike that of body waves. This study aims not only to alleviate the Lamb wave dispersion characteristics but also to perform a full reconstruction of the input signals via wavelet-based signal processing techniques.

## Time Reversibility of Lamb Waves in a Thin Plate

Once a response signal due to the original input signal at PZT patch A is measured at PZT patch B, the reconstructed input signal at PZT patch A of Figure 3 can be obtained by reemitting the response signal at PZT patch B with the signals being reversed in time. Note that the time reversal operation of a signal in a time domain can be represented as the complex conjugate of the signal in a frequency domain. Therefore, the time reverse operation of the response signal in the time domain at PZT patch B is equivalent to the complex conjugate of Eq.(3) in the frequency domain.

$$\hat{V}_B^*(r,\omega) = K_s^*(\omega)\hat{\mathrm{E}}_B^*(r,\omega) \tag{6}$$

where, a superscript $^*$ denotes a complex conjugate.

The reconstructed signal at PZT patch A from the reemitted signal at PZT patch B can be represented in a similar fashion as Eq. (3).

$$\hat{V}_A(r,\omega) = K_s(\omega)\hat{\mathrm{E}}_A(r,\omega) \tag{7}$$

where

$$\hat{\mathrm{E}}_A(r,\omega) = \hat{V}_B^*(\omega)K_a(\omega)G(r,\omega) \tag{8}$$

Using Eqs.(4), (6) and (8), the reconstructed signal in Eq.(7) can be rewritten as follows.

$$\hat{V}_A(r,\omega) = \hat{I}_A^*(\omega)K_a^*(\omega)K_s^*(\omega)K_a(\omega)K_s(\omega)G(r,\omega)G^*(r,\omega) \tag{9}$$

Performing an inverse Fourier transform, the reconstructed input signal $\widetilde{V}_A$ at PZT patch A can be obtained in the time domain as:

$$\widetilde{V}_A(t) = \frac{1}{2\pi}\int_{-\infty}^{\infty}\hat{I}_A^*(\omega)K_{as}^*(\omega)K_{as}(\omega)G^*(r,\omega)G(r,\omega)e^{i\omega(T-t)}d\omega \tag{10}$$

where, $K_{as}$ denotes the product between $K_a$ and $K_s$, and $T$ represents the total time period for the signal. If the time reversibility of waves were satisfied, the reconstructed signal $\widetilde{V}_A(t)$ in Eq.(10) would be identical to the time-reversed original signal $I_A(T-t)$. To directly compare with the original input signal $I_A(t)$ at PZT patch A, Eq.(10) should be shifted as:

$$\tilde{V}_A(T-t) = \frac{1}{2\pi}\int_{-\infty}^{\infty} \hat{I}_A(\omega) K_{TR}(\omega) G_{TR}(r,\omega) e^{-i\omega t} d\omega \tag{11}$$

where,

$$\begin{aligned} K_{TR}(\omega) &= K_{as}(\omega) K_{as}^*(\omega) \\ G_{TR}(\omega) &= G(r,\omega) G^*(r,\omega) \end{aligned} \tag{12}$$

Here, $K_{TR}$ is a constant determined by the electro-mechanical efficiency of the PZT patch, and $G_{TR}$ is referred to as a time reversal operator of Lamb waves in the Mindlin plate theory. In Equation (12), the time reversibility is achieved only if $K_{TR}$ and $G_{TR}$ are independent of the angular frequency $\omega$. That is, for the time reversal operation, the wave components at different frequency values should be uniformly amplified throughout the whole frequency range. As shown in Figure 4, for Lamb wave propagation, however, the time reversal operator $G_{TR}$ varies with response to frequency, indicating that the wave components at different frequency values are non-uniformly amplified. Therefore, the original input signal cannot be properly reconstructed if a broadband input signal is used.

To alleviate this problem, a narrow-band excitation signal incorporated with a signal processing based on a multi-resolution analysis is employed in this study so that the time reversibility of the reconstructed signals can be preserved within an acceptable tolerance. Note that when a single frequency input is used, the frequency dependency shown in Equation (12) disappears, allowing proper reconstruction of the original input signal. In Section 4, the time reversibility is further improved by incorporating a well-designed narrowband input waveform with the wavelet transform.

**Application of Time Reversal Lamb Waves to Delamination Detection in a Composite Plate**

Intact composites possess atomic linear elasticity as water and copper do. The atomic elastic material is well described by the classical linear elastic constitutive law and linear wave propagation equations. However, it should be noted that the atomic elastic materials demonstrate nonlinear mesoscopic elasticity that appears to be much like that in rock or concrete if they have been damaged. Nonlinear mesoscopic elastic materials have hysteretic nonlinear behaviors yielding acoustic and ultrasonic wave distortion, which gives rise to changes in the resonance frequencies as a function of drive amplitude, generation of accompanying harmonics, nonlinear attenuation, and multiplication of waves in different frequencies [14,15]. It has been also shown that cracks and delamination with low-aspect-ratio geometry are the scattering sources creating nonclassical nonlinear waves, which arise from hysteresis in the wave pressure-deformation relation [16]. Wave scattering can be also caused by either horizontal or vertical mode conversion in which the energy of the incident Lamb waves at a specified driving frequency is redistributed into neighboring Lamb wave modes as shown in Figure 2. Because delamination changes the internal geometric boundary conditions in a composite plate, diffraction and reflection of the waves can also produce wave scattering when the incident Lamb waves pass through delamination.

Because the time reversibility of waves is fundamentally based on the linear reciprocity of the system [10,11], the linear reciprocity and the time reversibility break down if there exists any source of wave distortion due to wave scattering along the wave path. Therefore, by comparing the discrepancy between the original input signal and the reconstructed signal, damage such as crack opening-and-closing, delamination and fiber breakage could be detected.

In most of conventional damage detection techniques, damage is inferred by comparing newly obtained data sets with baseline data previously measured from an initial condition of the system. Because there might have been numerous variations since the baseline data were collected, it would be difficult to blame structural damage for all changes in the measured signals. For instance, there might have been operational and environmental variation of the system once the baseline data have been collected. Therefore, data normalization, which attempts to distinguish signal changes originated from structural damage from those caused by natural variations of the system, needs to be addressed [17].

In this study, the dependency on the baseline data measured at some previous time point is completely eliminated by instantly comparing the original input signal and the reconstructed input signal. Furthermore, the active PZT sensing system employed in this study allows an easy implementation of the time reversal process. The generation of the input signal, excitation of the actuation PZT, and acquisition of the response signal are fully automated, and the entire time reversal process for one particular path takes less than a minute.

## 4. AN ENHANCED TIME REVERSAL METHOD USING WAVELET SIGNAL PROCESSING

In the previous section, we have described the basic concept of time reversal analysis for Lamb wave propagation based on Mindlin plate theory. In this section, we discuss the use of wavelet-based signal processing techniques to enhance the time reversibility of Lamb waves in the presence of background noise.

### Active Sensing using a Known Input Waveform

First, a carefully designed narrowband input waveform is exerted onto a structure to minimize the frequency dependency of the time reversal operator and to maintain high signal-to-noise ratio of the time reversal process. The advantage of using the narrowband input signal is to prevent the time reversal operator in Eq (12) from having large variations around the driving frequency. In addition, the use of a known and repeatable input further makes the subsequent signal processing for the time reversal process much easier and repeatable. A similar approach to noise elimination in ultrasonic signals for flaw detection can be found in [18]. A Morlet wavelet function, as defined below, with a driving frequency around a specified narrowband frequency range is adopted as an input waveform [19].

$$\Psi(t) = \mathrm{e}^{-t^2/2}\cos(5t) \tag{13}$$

A proper selection of the driving frequency is critical for successful generation of Lamb waves in a given structure. Further discussion on the selection of the driving frequency can be found in Sohn et al. 2004 [17].

**Automated Signal Selection Process based on Wavelet Transform**

As discussed in Section 2, the time reversal analysis based on the Mindlin plate theory is limited only to the $A_0$ mode. However when Lamb waves travel in a thin plate, a response signal consists of several wave modes as illustrated in Figure 5. Some of the modes are symmetric modes associated with the direct path of wave propagation and/or signals reflected off from the edges of the plate. There are also additional anti-symmetric modes reflected off from the edges. Because these reflected modes are very sensitive to the changes in boundary conditions, our primary interest lies in investigating the $A_0$ mode corresponding only to the direct path between the actuating PZT and the sensing PTZ. Note that this $A_0$ mode traveling along the direct path between the actuator and the sensor is insensitive to changing boundary conditions. Therefore, only the $A_0$ mode portion of the signal needs to be extracted from the raw signal to minimize false warnings of damage due to changing operational conditions of the system. Because this signal component of our interest, the $A_0$ mode, is time and frequency limited, the two-dimensional time-frequency representation of the signal can be a useful tool for simultaneous characterization of the signal in time and frequency, in particular for characterizing dispersive effects and analyzing multimodal signals. For this purpose, an automated selection procedure based on wavelet analysis is developed.

The basic concept of this automated selection procedure is as follows: If the signal shape that needs to be extracted for damage detection is known *a priori*, optimal extraction can be achieved using a matched mother wavelet that models the shape of the signal component [20]. The automated selection procedure is schematically shown in Figure 6. First, the continuous wavelet transform of the signal, $Wf(u,s)$, is obtained by convolving the signal *f(t)* with the translations ($u$) and dilations ($s$) of the mother wavelet:

$$Wf(u,s) = \int_{-\infty}^{\infty} f(t) \frac{1}{\sqrt{s}} \psi^*_{u,s}(t)\, dt \qquad (14)$$

where

$$\psi^*_{u,s}(t) = \frac{1}{\sqrt{s}} \psi\left(\frac{t-u}{s}\right) \qquad (15)$$

The Morlet wavelet, same as the previously defined input signal, is used as a mother wavelet $\Psi(t)$ for wavelet transform. Then a complete set of daughter wavelets $\psi^*_{u,s}(t)$ is generated from the mother wavelet by the dilation ($s$) and shift ($u$) operations. Note that each value of the wavelet coefficient $Wf(u,s)$ is normalized by the factor $1/\sqrt{s}$ to ensure that the integral energy given by each wavelet is independent of the dilation $s$.

Because the Morlet wavelet is used as a mother wavelet for wavelet transform and the wavelet coefficient is the correlation between the signal and the mother wavelet by definition, the wavelet coefficient arrives at its maximum value when the shape of the response signal becomes closest to that of the Morlet wavelet. When this search of the maximum wavelet coefficient is performed at the input frequency, the time portion of the $A_0$ mode can be easily detected by the temporal shift parameter $u$. Hence, this wavelet transform can be an effective way to reduce noise if the mother wavelet is chosen to be a good representation of the signal to be detected. Furthermore, the continuous wavelet transform is performed instead of the discrete wavelet transform to obtain a better time resolution over the full period of the signal [21]. Through this automated selection procedure, only the $A_0$ mode of the response time signal is chosen for reemission. This selection procedure also automatically eliminates the portion of the response signal contaminated by electromagnetic interference.

**Signal Filtering based on Multi-Resolution Analysis**

When a narrowband signal travels through a thin solid media, the dispersive nature of the wave can be compensated through the conventional time reversal process. In other words, the time reversal process compensates a phase difference of each wave packet in a frequency domain by reemitting each wave packet with proper time delays. However, the frequency content of the traveling waves smears into nearby frequencies and is non-uniformly amplified during the time reversal process. Therefore, to enhance the time reversibility of the reconstructed signal at the original input point, the measured response signal needs to be processed before reemitting at the response point. In particular, for the time reversal analysis of Lamb waves, it is critical to retain the response components only at the original input frequency value, because of the frequency dependent nature of the time reversal operator shown in Figure 4. To achieve this goal, a multi-resolution analysis is adopted to filter out the measurement noise in response signals and to keep only the response component at the driving frequency value. Multi-resolution signal processing based on wavelet transform has been extensively studied especially for perfect reconstruction of signals using quadrature mirror filters [22].

Once the wavelet coefficients are computed from Eq.(14), the original signal can be reconstructed via the following inverse continuous wavelet transform [22]:

$$f(t) = \frac{1}{C_{\varphi}} \int_{-\infty}^{\infty}\int_{0}^{\infty} Wf(u,s)\, \frac{1}{\sqrt{s}}\, \psi\!\left(\frac{t-u}{s}\right) \frac{1}{s^{2}}\, ds\, du \tag{16}$$

where $C_{\varphi}$ is a constant determined by

$$C_{\psi} = \int_{0}^{\infty} \frac{|\psi|}{\omega}\, d\omega \tag{17}$$

In this study, the integration operation with respect to the scale parameter $s$ in Eq. (16) is restricted only to near the driving frequency in order to filter out frequency components outside the driving frequency before transmitting the response signal back to the original input location:

$$f(t) = \frac{1}{C_{\varphi}} \int_{-\infty}^{\infty}\int_{a}^{b} Wf(u,s)\, \frac{1}{\sqrt{s}}\, \psi\!\left(\frac{t-u}{s}\right) \frac{1}{s^{2}}\, ds\, du \tag{18}$$

where $a$ and $b$ are the lower and upper limits of the narrowband excitation frequency. The choice of the frequency limits is dictated by the fact that the filter must cover the frequency range of interest so that useful information is not lost. In fact, the wavelet transform is used as a matched filter to improve the signal-to-noise ratio without any loss in time resolution or accuracy and in many cases with improvements. This filtering processing is repeated for the reconstructed input signal obtained by the time reversal process. An example of this filtering process is shown in Figure 7. It can be seen that the filtering process reconstructs the raw response signal after removing frequency components outside the excitation frequency.

## 5. EXPERIMENTAL STUDY

The overall test configuration of this study is shown in Figure 8(a). The test setup consists of a composite plate with a surface mounted sensor layer, a personal computer with a built-in data acquisition system, and an external signal amplifier. The dimension of the composite plates is 60.96 cm x 60.96 cm x 0.6350 cm (24 in x 24 in x 1/4 in). The layup of this quasi-isotropic plate contains 48 plies stacked according to the sequence $[6(0/45/-45/90)]_S$, consisting of Toray T300 Graphite fibers and a 934 Epoxy matrix.

A commercially available thin film with embedded piezoelectric (PZT) sensors is mounted on one surface of the composite plate as shown in Figure 8(b) [23]. A total of 16 PZT patches are used as both sensors and actuators to form an "active" local sensing system. Because the PZTs produce an electrical charge when deformed, the PZT patches can be used as dynamic strain gauges. Conversely, the same PZT patches can also be used as actuators, because elastic waves are produced when an electrical field is applied to the patches. These PZT sensor/actuators are inexpensive, generally require low power, and are relatively non-intrusive.

The personal computer shown in Figure 8(a) has built-in analog-to-digital and digital-to-analog converters, controlling the input signals to the PZTs and recording the measured response signals. Increasing the amplitude of the input signal yields a clearer signal, enhancing the signal-to-noise ratio. On the other hand, the input voltage should be minimized for field applications, requiring as low power as possible. In this experiment the optimal input voltage was designed to be near 45 V, producing 1-5 V output voltage at the sensing PZTs. For the time reversal analysis, the measured response signal is amplified before being reemitted to the original source point. PZTs in a circular shape are used with a diameter of only 0.64 cm (1/4 in). The sensing spacing is set to 15.24 cm (6 in). A discussion on the selection of design parameters such as the dimensions of the PZT patches, sensor spacing, and a driving frequency can be found in [24].

The strain responses measured from the experimental study and simulated by the Mindlin plate theory are compared in Figure 9 for a wave propagation path corresponding to the actuating PZT #15 and the sensing PZT #16. The measured strain response corresponding to the first flexural $A_0$ mode is well-predicted by the Mindlin plate theory as shown in Figure 9. It should be reminded that because the Mindlin plate theory, which approximate the Rayleigh-Lamb equations for an infinite plate, is used to predict only the wave propagation of the $A_0$ mode corresponding to the direct path between the actuating and sensing PZTs, the additional wave modes reflected off from the boundaries of the plate are not predicted by the Mindlin plate theory. The simulated strain response is obtained from Eqs. (4) and (5). The elasticity modulus and Poisson ratio are approximated by assuming a quasi-isotropic composite plate [2]. It should be noted that the approximated elasticity modulus and Poisson ratio are properly calibrated so that the arrival time of the simulated and measured waves coincides. Without calibration, it is observed that the simulated wave travels slightly slower than the measured wave while the shape of the simulated and the measured waves are almost identical.

Figure 10 illustrates the typical results of the enhanced time reversal method obtained from the composite plate used in this study. First, one PZT patch is designated as an actuator, exerting a predefined waveform into the structure [Figure 10(a)]. Then, an adjacent PZT become a strain sensor and measures a response signal [Figure 10(b)]. Once the traveled waves are measured at the response point, the measured signal is processed using the wavelet-based signal processing procedures described in Section 4: First, the $A_0$ segment of the response signal is selected via the proposed autonomous selection scheme. Then, the wavelet-based filtering is applied to the response signal to retain only the response component at the driving frequency. Figure 10(c) shows the $A_0$ mode selected from the response signal in Figure 10(b) after being filtered and reversed in a time domain. This processed response signal is reemitted from the previous sensing PZT, which is now an actuator. The reconstructed response signal at the original input PZT location is shown in Figure 10(d). This process of the Lamb wave propagation and the time reversal analysis is repeated for different combinations of actuator-sensor pairs. A total of 66 different path combinations are investigated. Finally, the original input signal and the reconstructed signal at the original input point are compared for the actuation PZT #1 and the sensing PZT #6 in Figure 11.

Our ultimate goal is to estimate damage by comparing the shape of the original input signal and that of the reconstructed signal. Figure 11 demonstrates that the initial input waveform is well restored through the enhanced time reversal method when there is no defect in the composite plate tested. However, our destructive testing of the composite plate reveals that this time reversibility is violated once damage is introduced along the wave propagation path. Typical indications of damage include appearance of sub- and super-harmonic frequency components, signal attenuation and distortion. A current research is underway to classify damage into several types based on these distinctive changes in the reconstructed signal.

One potential advantage of the time reversal analysis is that damage might be inspected without requiring any baseline data to be obtained at some previous time point. This advantage over conventional damage detection techniques allows minimizing false warnings of damage. For instance, if the operational temperature or boundary conditions of a system change after the baseline data are collected, most pattern recognition techniques will have difficulties in discerning signal changes caused by damage from those due to the temperature or boundary condition changes. In other words, if there are any changes in the newly measured signal since the baseline signal is obtained, it is hard to determine what is causing this change. However, by instantly comparing the input waveform with the reconstructed signal, the time dependent issue of the conventional pattern recognition techniques can be eliminated, making it much easier to distinguish signal changes caused by damage from those caused by natural variation of the system.

## 6. SUMMARY AND DISCUSSION

In this study, the applicability of a time reversal method to health monitoring of a composite plate is investigated. In particular, a unique input waveform and signal processing techniques are employed to improve the time reversibility of Lamb waves. First, a narrowband excitation waveform is employed to address the frequency dependency of the time reversal operator. Then, an automated signal selection process is developed based on wavelet transform to retain only a segment of a raw response signal that is more sensitive to damage and less responsive to changing boundary conditions. In addition, a wavelet-based filtering is performed to further enhance the time reversibility by taking advantage of temporal and spectral differences between the signal component of our interest and background noise. Using an active sensing system mounted on a composite plate, it has been demonstrated that an input waveform exerted at an actuating PZT can be reconstructed at the excitation point after processing the response signal measured at a distance from the excitation point and reemitting the processed signal at the sensing location with being reversed in a time domain. Because the reconstructed signal is expected to be identical to the original input signal for a system with no defects, this time reversibility of Lamb waves will allow detecting damage by comparing a known input waveform with a reconstructed signal.

Many uncharted applications of this time reversal analysis to structural health monitoring no doubt lie in wait. A continuous research is currently underway to classify different representative damage types based on distortion characteristics between the input waveform and the reconstructed signal. Further research is also warranted to optimally design the parameters of the active sensing system such as the spacing between the PZT patches, the actuating frequency, and power requirement for the PZTs. It should be pointed out that the procedure developed in this study has only been verified on a relatively simple laboratory test specimen. To fully verify the proposed approach, it will be necessary to apply the proposed approach to different types of representative structures.

## 7. ACKNOWLEDGMENTS

This research is partially sponsored by Los Alamos National Laboratory, Contract Number 75067-001-03. Funding for this project has been provided by the Department of Energy through the internal funding program at Los Alamos National Laboratory known as Laboratory Directed Research and Development (Damage Prognosis Solutions). Additional support has been provided from the National Science Foundation, Grant Numbers CMS-9988909. The first author would like to acknowledge the Post-doctoral Fellowship Program of Korea Science & Engineering Foundation (KOSEF), which provides support for his stay at Stanford University.

## REFERENCE

[1] E.Moulin, J.Assaad, C.Delebarre H.Kaczmarek, D.Balageas, Piezoelectric transducer embedded in a composite plate: application to Lamb wave generation. *Journal of Applied Physics*, 82(5) (1997), 2049-2055.

[2] H.Sohn, G.Park, J.R.Wait., N.P.Limback, C.R.Farrar, Wavelet-based active sensing for delamination detection in composite structures. *Smart Materials and Structures*, 13(1) (2004) 153-160.

[3] C.A.Paget, S.Grondel, K.Levin, C.Delebarre, Damage assessment in composites by Lamb waves and wavelet coefficients. *Smart Materials and Structures*, 12(3) (2003) 393-402.

[4] S.S.Kessler, C.E.Johnson, C.T.Dunn, Experimental application of optimized Lamb wave actuating/sensing patches for health monitoring of composite structures, *Proceedings of the 4th International Workshop on Structural Health Monitoring*, Stanford University, 2003, pp. 429-436

[5] C.H.Wang, J.T.Rose, F.K.Chang, A computerized time-reversal method for structural health monitoring. *Proceedings of SPIE Conference on Smart Structures and NDE*, San Diego, CA, USA, 2003

[6] C.Prada, M.Fink, Separation of interfering acoustic scattered signals using the invariants of the time-reversal operator. Application to Lamb waves characterization. *J. Acoust. Soc. Am.*, 104(2) (1998) 801-807.

[7] R.K.Ing, M.Fink, Time recompression of dispersive Lamb waves using a time reversal mirror – Application to flaw detection in thin plates, *1996 IEEE Ultrasonics Symposium*, 1 ,1996, 659-663.

[8] R.K.Ing, M.Fink, Time-reversed Lamb waves. *IEEE Transactions on Ultrasonics, Ferroelectrics, and Frequency control*, 45(4) (1998) 1032-1043.

[9] M.Fink, Time-reversed acoustics. *Scientific American*, 281(5) (1999) 91-97.

[10] C.Draeger, D.Cassereau, M.Fink, Theory of the time-reversal process in solids. *J. Acoust. Soc. Am.*, 102(3) (1997) 1289-1295.

[11] M.Fink, C.Prada, Acoustic time-reversal mirrors. *Inverse Problems*, 17 (2001) R1-R38.

[12] I.A.Viktorov, *Rayleigh and Lamb Waves*, Plenum Press: New York, 1967.

[13] L.R.F.Rose, C.H.Wang, Mindlin plate theory for damage detection I, source solutions. *J. Acoust. Soc. Am.*, (2003) in press.

[14] R.A.Guyer, P.A.Johnson, Nonlinear mesoscopic elasticity : Evidence for a new class of materials. *Physics Today*, April (1999) 30-36.

[15] K.V.D.Abeele, P.A.Johnson, A.Sutin, Nonlinear elastic wave spectroscopy (NEWS) techniques to discern material damage, part I : Nonlinear wave modulation spectroscopy (NWMS). *Res Nondestr. Eval.*, 12 (2000) 17-30.

[16] V.V.Kazakov, A.Sutin, P.A. Johnson, Sensitive imaging of an elastic nonlinear wave-scattering source in a solid. *Applied Physics Letters*, 81(4) (2002) 646-648.

[17] H.Sohn, Effects of environmental and operational variability on structural health monitoring. *submitted for publication of a Special Issue of Philosophical Transaction of Royal Society on Structural Health Monitoring* (2004).

[18] A.Abbate, J.Koay, J.Frankel, S.C.Schroeder, P.Das, Signal detection and noise suppression using a wavelet transform signal processor: Application to ultrasonic flaw detection. *IEEE Transactions on Ultrasonics, Ferroelectrics, and Frequency Control*, 44(1) (1997) 14-26.

[19] G.Strang, T. Nguyen, *Wavelets and Filter Banks*, Wellesley-Cambridge Press:Wellesley MA, 1997.

[20] P.Das, *Optical Signal Processing: Fundamental*, Springer-Verlag: New York NY, 1991.

[21] C.S.Burrus, R.A.Gopinath, H.Guo, *Introduction to Wavelets and Wavelet Transforms*, Prentice Hall: Upper Saddle River, New Jersey 07458, 1998.

[22] A.N.Akansu, R.A.Haddad, *Multiresolution Signal Decomposition*, Academic Press: San Diego CA, 1992.

[23] http://www.acellent.com.

[24] S.S.Kessler, Piezoelectric-based In-situ Damage Detection of Composite Materials for Structural Health Monitoring Systems, Ph.D. Thesis, MIT, Massachusetts, 2002.

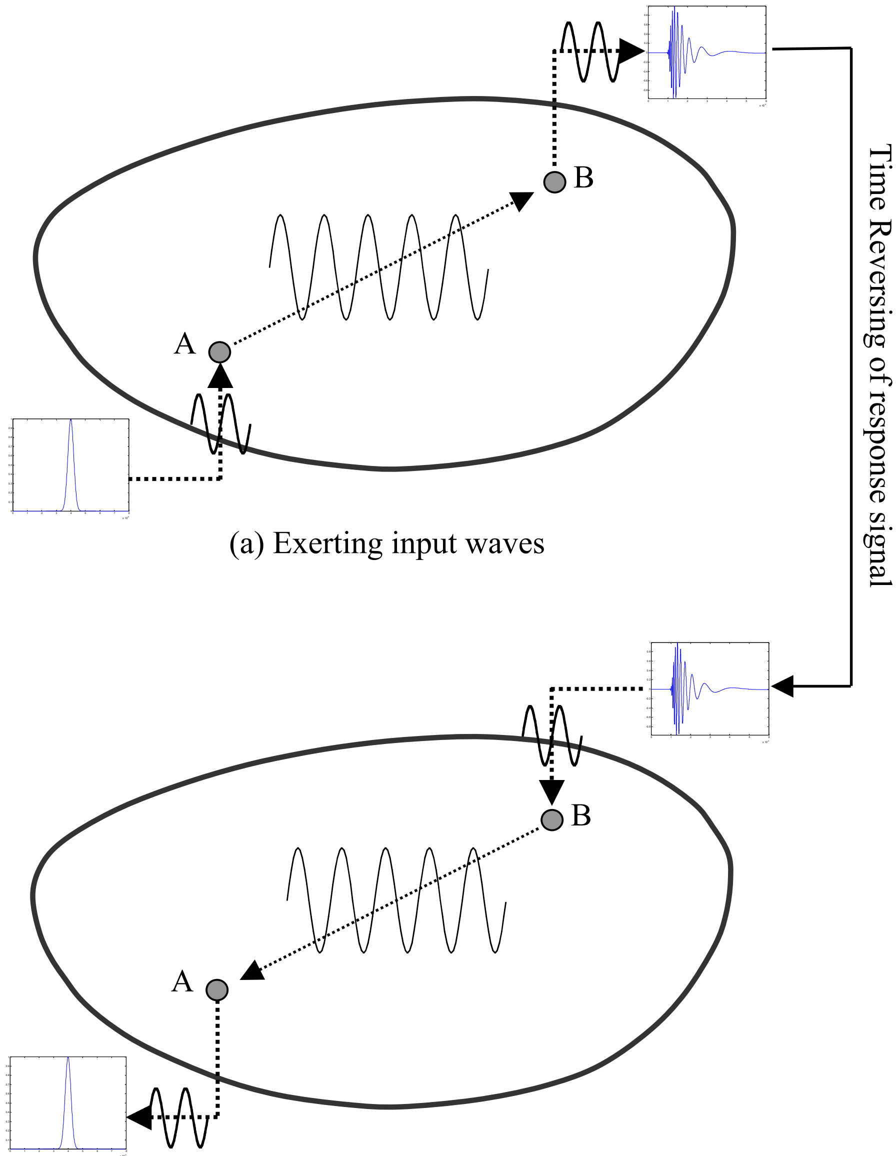


(a) Exerting input waves

(b) Reemitting response waves being reversed with time

Figure 1: Time reversal concept

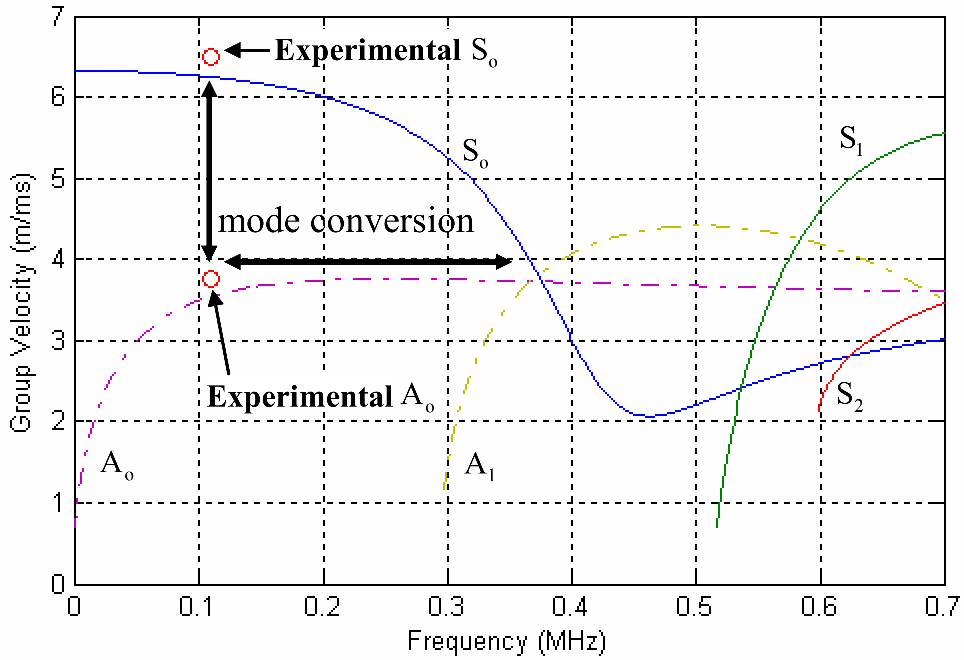

Figure 2: A dispersion curve for an idealized isotropic composite plate (the abscissa is presented in term of the frequency with the constant plate thickness (0.64 cm) rather than the frequency-thickness product)

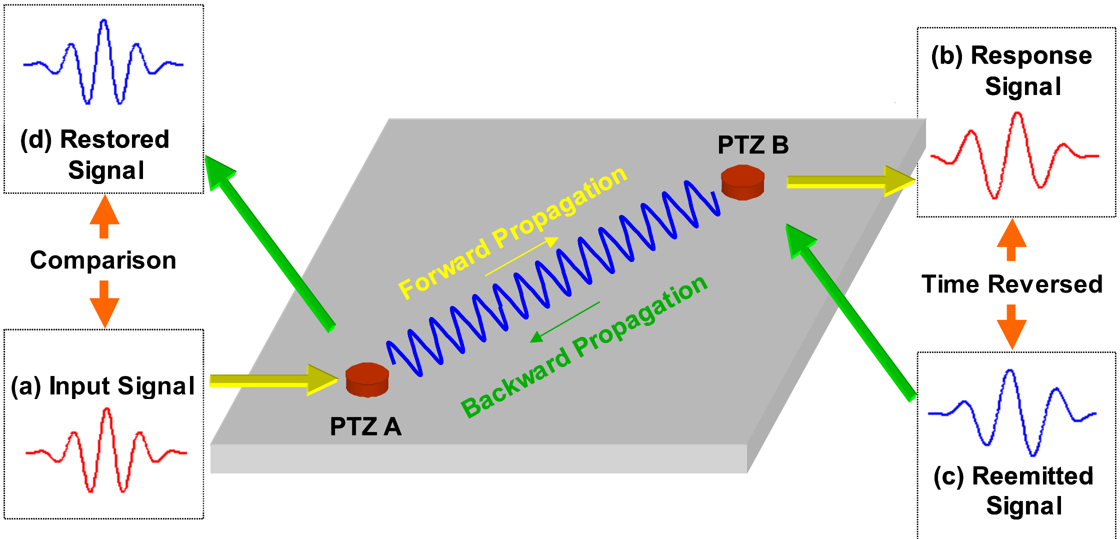


Figure 3: Generation and Sensing of Lamb waves on a plate by using PZT patches

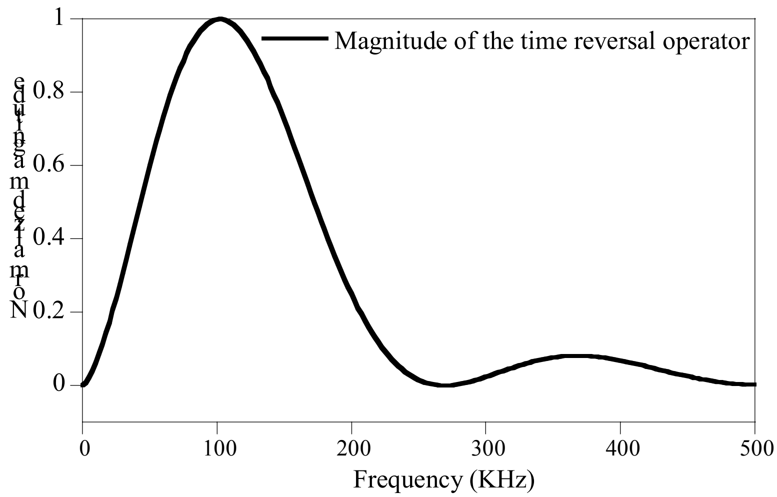


Figure 4: Normalized time reversal operator of the $A_0$ mode

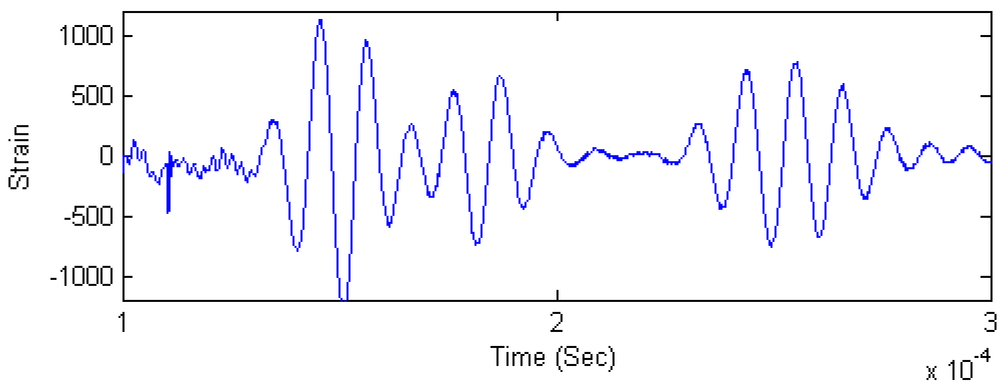

Figure 5: A typical dynamic strain response measured at one of the piezoelectric sensors

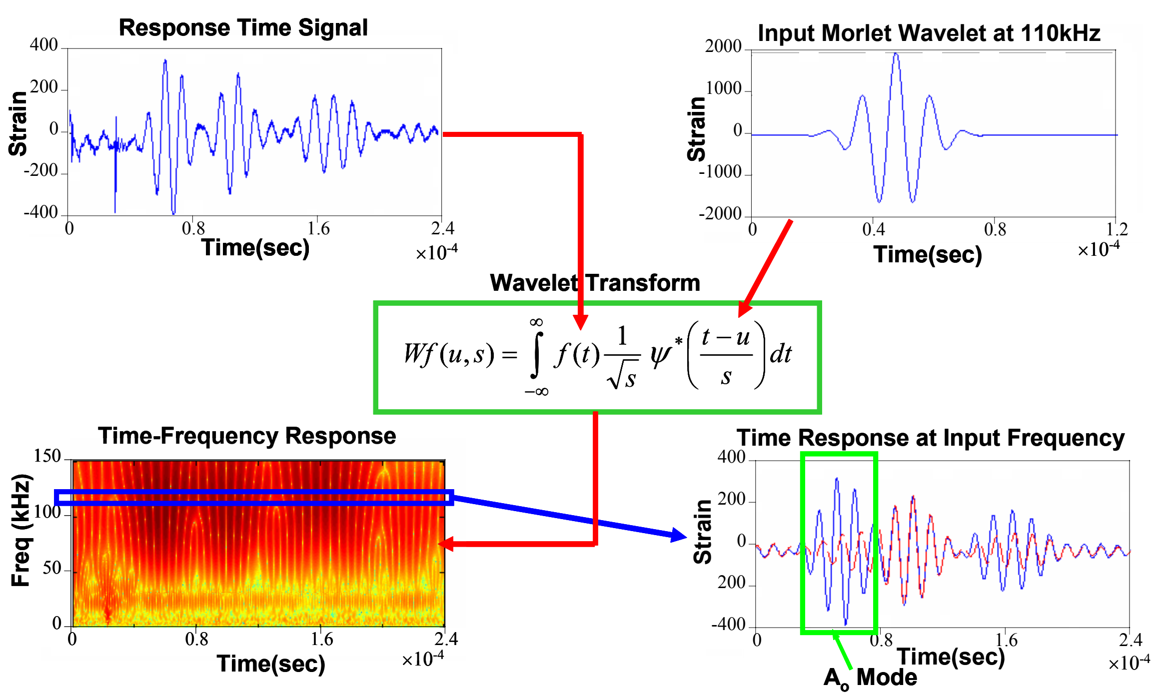


Figure 6: A wavelet analysis procedure for automated signal selection

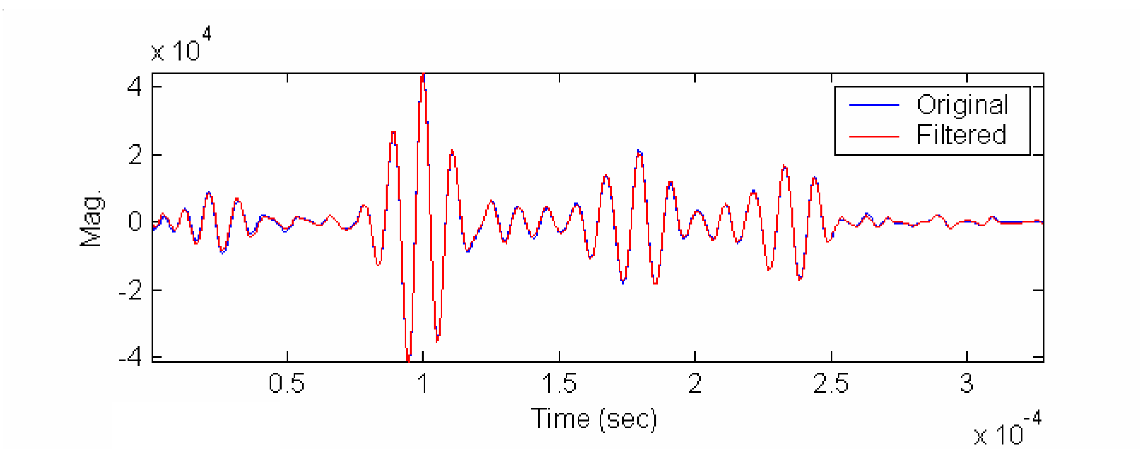


Figure 7 : Comparison between the raw signal and the restored signal after filtering

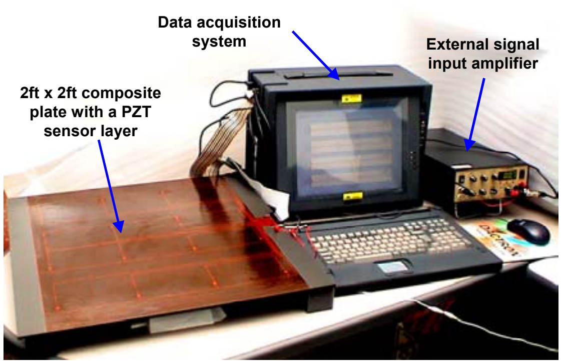


(a) Testing configuration

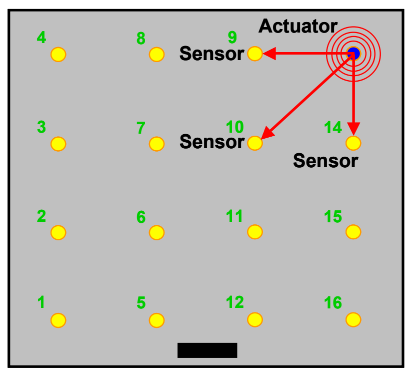


(b) A layout of the PZT sensors/actuators

Figure 8 : An active sensing system for detecting delamination on a composite plate

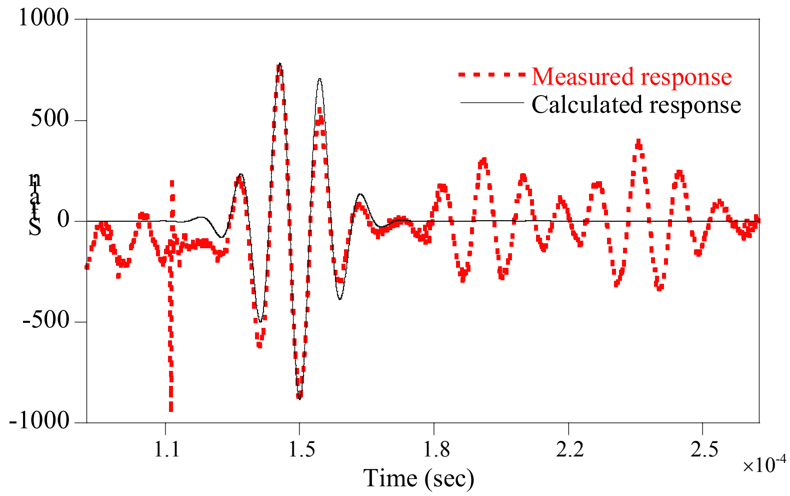


Figure 9: Comparison between the calculated and the measured strain response of the path from PZT#15 to PZT#16

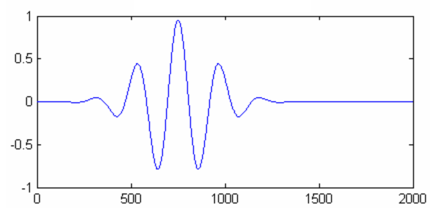

(a) An original input Morlet waveform

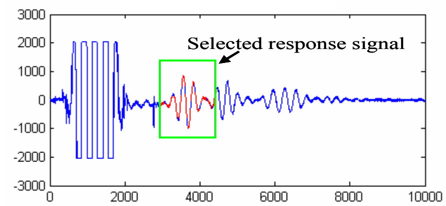


(b) A response signal at a sensing PZT

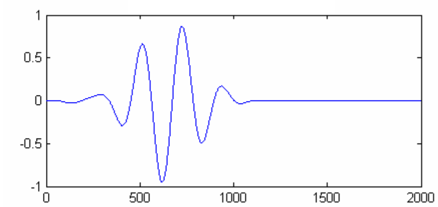

(c) A time-reversed response signal after signal processing

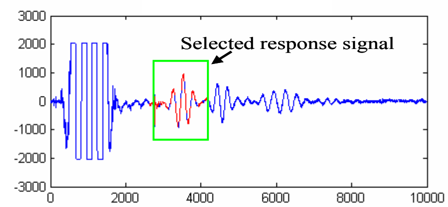


(d) A response signal at the original actuating PZT

Figure 10 : Measured time signals at various stages of the time reversal analysis

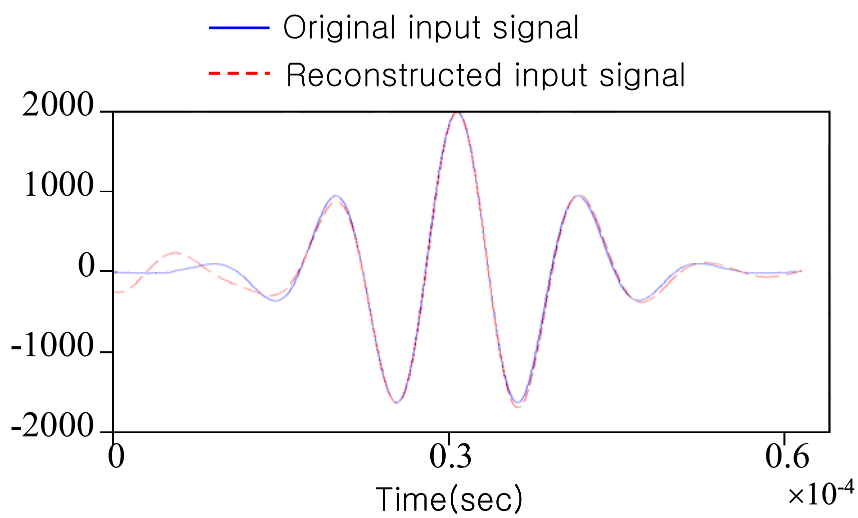


Figure 11: Comparison between the original input signal (solid) and the restored signal (dotted) after the automated selection and filtering